

# CONTINUUM MODELING OF INTERFACIAL LOAD TRANSFER IN CARBON NANOTUBE/POLYMER COMPOSITES SUBJECTED TO TENSION AND BENDING

Konstantinos I. TSERPES<sup>1</sup>, Paraskevas PAPANIKOS<sup>2</sup>, Spyros PANTELAKIS<sup>1</sup>

<sup>1</sup>Dept. of Mechanical Engineering & Aeronautics, University of Patras, Patras, 26500, Greece

<sup>2</sup>Dept. of Product & Systems Design Engineering, University of the Aegean, Syros, 84100, Greece

**Keywords:** Carbon nanotubes, Representative volume element, Continuum modeling, Finite element analysis, Composite materials

## 1 INTRODUCTION

Combining superior mechanical properties and fiber-like structure, carbon nanotubes (CNTs) offer unique potential for reinforcing polymers either as replacements of conventional fibers or as fillers to enhance the properties of the existed advanced composites. Reinforcing effectiveness is critically controlled by the interfacial load transfer between the nanotube and the polymer. Actually, in composites, the constituents do not dissolve or merge completely and therefore, normally, exhibit an interface between one another, which can be considered as a different material with different mechanical properties. Mechanical characteristics (elastic modulus, tensile strength and fracture toughness) of composites greatly depend on the mechanical load transfer from the matrix to the nanotube. As an example, if the composite is subjected to tensile loading and there exists perfect bonding between the nanotube and polymer and/or a strong interface then the load (stress) is transferred to the nanotube; since the tensile strength of the nanotube (or the interface) is very high the composite can withstand high loads. However, if the interface is weak or the bonding is poor, on application of high loading either the interface fails or the load is not transferred to the nanotube and the polymer fails due to their lower tensile strengths. Consider another example of transverse crack propagation. When the crack reaches the interface, it will tend to propagate along the interface, since the interface is relatively weaker (generally) than the nanotube (with respect to resistance to crack propagation). If the interface is weak, the crack will cause the interface to fracture and result in failure of the composite. In this aspect, CNTs are better than traditional fibers (glass, carbon) due to their ability to inhibit nano and micro cracks. Hence, the knowledge and understanding of the nature and mechanics of load (stress) transfer between the nanotube and polymer and properties of the interface is critical for manufacturing of mechanically enhanced CNT–polymer composites and will enable in tailoring of the interface for specific applications or superior mechanical properties.

Generally, interfacial mechanics of CNT–reinforced composites is appealing from three aspects: mechanics, chemistry, and physics. From the mechanics point of view, the important aspects are [1]: (a) the relationship between the mechanical properties of individual constituents, i.e. nanotube and polymer, and the properties of the interface and the composite overall, and (b) the ability of the modeling to estimate the properties of the composites for the design process for structural applications.

Aiming to contribute towards resolution of these aspects, we present herein a continuum approach for modeling the interfacial load transfer between the nanotube and polymer matrix. The approach is incorporated into a multi-scale finite element-based representative volume element (RVE).

## 2 THE MULTI-SCALE RVE

The synthesis of the multi-scale RVE is shown in Figure 1. Initially, the isolated nanotube is simulated using an equivalent beam possessing the same tensile, bending and torsional behavior with the nanotube itself. Equivalent properties (geometrical characteristics and elastic moduli) are evaluated by combining atomistic-based FE analysis with mechanics of materials. Then, the equivalent beam is inserted into the matrix to form the RVE. Between the beam and the matrix a hollow cylinder, playing the role of the interface, is placed. Each of the above steps is described in details in the following sections.

The concept of the multi-scale RVE was initially presented in Ref. [2]. In regard of these works, herein, we introduce the equivalent beam concept and continuum modeling of the interface between the nanotube and the matrix enabling the study of the influence of interfacial properties on the bulk mechanical behavior of CNT/polymer composites.

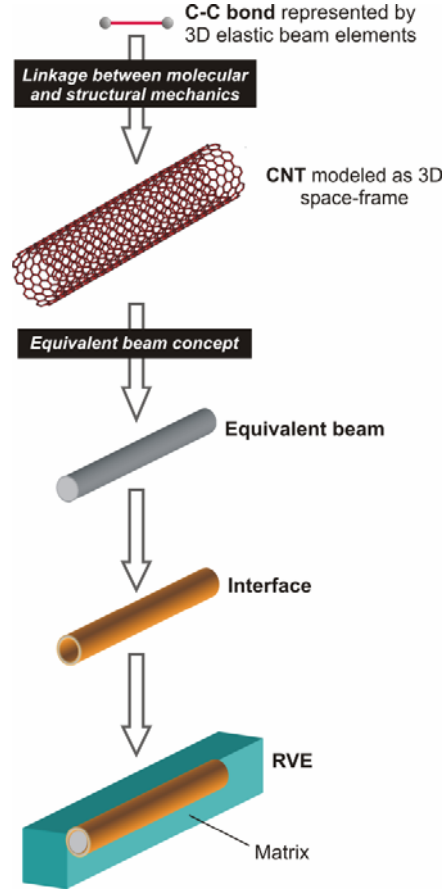


Fig.1: Synthesis of the multi-scale RVE.

## 2 THE EQUIVALENT BEAM CONCEPT

The concept of the 'equivalent beam' is based on the condition of identical mechanical behavior between the CNT and the beam, which corresponds to identical tensile, bending and torsional behaviors. As for elastic beams, these behaviors are designated by the corresponding rigidities and in order to fully define the equivalent beam, it suffices to evaluate its equivalent properties (geometrical characteristics and elastic moduli) from the nanotube's rigidities.

In order to derive the nanotube's rigidities, a 3D FE model has been used. The model treats CNTs as space-frame structures. Using 3D elastic beam elements, the exact atomic structure of the nanotubes is modeled. The elastic moduli of the beam elements are determined using a linkage between molecular and continuum mechanics. The following relationships between the structural mechanics parameters and the molecular mechanics parameters are obtained

$$\frac{E_b A_b}{\ell} = k_r, \quad \frac{E_b I_b}{\ell} = k_\theta, \quad \frac{G_b J_b}{\ell} = k_\tau \quad (1)$$

Here,  $\ell$  is the bond length equal to 0.1421 nm;  $E_b$  and  $G_b$  are the bond's Young's modulus and shear modulus, respectively;  $I_b$  and  $J_b$  are the moment of inertia and polar moment of inertia, respectively, and  $k_r$ ,  $k_\theta$ , and  $k_\tau$  are the bond stretching, bond bending and torsional resistance force constants, respectively. Assuming a solid circular cross-sectional area of the beams with diameter  $d$  and setting  $A_b = \pi d^2 / 4$ ,  $I_b = \pi d^4 / 64$  and  $J_b = \pi d^4 / 32$ , Eqs.(1) give

$$d = 4 \sqrt{\frac{k_\theta}{k_r}}, \quad E_b = \frac{k_r^2 \ell}{4\pi k_\theta}, \quad G_b = \frac{k_r^2 k_\tau \ell}{8\pi k_\theta^2} \quad (2)$$

Eqs.(2) give all necessary input parameters for the beam elements. In the present study, the following values were used for the force constants

$$k_r = 938 \text{ kcal mole}^{-1} \text{ \AA}^{-2} = 6.52 \times 10^{-7} \text{ N/nm}$$

$$k_\theta = 126 \text{ kcal mole}^{-1} \text{ rad}^2 = 8.76 \times 10^{-10} \text{ N nm/ rad}^2 = 0.876 \text{ nN nm rad}^{-2}$$

$$k_\tau = 40 \text{ kcal mole}^{-1} \text{ rad}^2 = 2.78 \times 10^{-10} \text{ N nm/ rad}^2 = 0.278 \text{ nN nm rad}^{-2}$$

Substituting the above values in Eqs.(2) and setting  $\ell = 0.1421 \text{ nm}$ , we obtain the input parameters for the beam elements:

$$d = 0.147 \text{ nm}, \quad E_b = 5488 \text{ nN nm}^{-2} = 5488 \text{ GPa}, \quad G_b = 870.7 \text{ nN nm}^{-2} = 870.7 \text{ GPa}$$

The cross-sectional area and moments of inertia are derived from the bond diameter

$$A_b = \frac{\pi d^2}{4} = 0.01688 \text{ nm}^2, \quad I_b = \frac{\pi d^4}{64} = 2.269 \times 10^{-5} \text{ nm}^4, \quad J_b = \frac{\pi d^4}{32} = 4.537 \times 10^{-5} \text{ nm}^4$$

However, since the modeling of the bond is done using beam elements, it is clear that the results of the analyses would be the same as long as the rigidities  $E_b A_b$ ,  $E_b I_b$ ,  $G_b J_b$  of the bond are the same. The constant values of the rigidities arise directly from Eqs.(1):

$$E_b A_b = 92.65 \text{ nN}, \quad E_b I_b = 0.1245 \text{ nN nm}^2, \quad G_b J_b = 0.0395 \text{ nN nm}^2$$

Since the nanotube possess a linear behavior, to derive the rigidities it is sufficient to apply in the FE model an arbitrary displacement such as to load the nanotube in tension, bending and torsion. The boundary and loading conditions for each case are depicted in Figure 2.

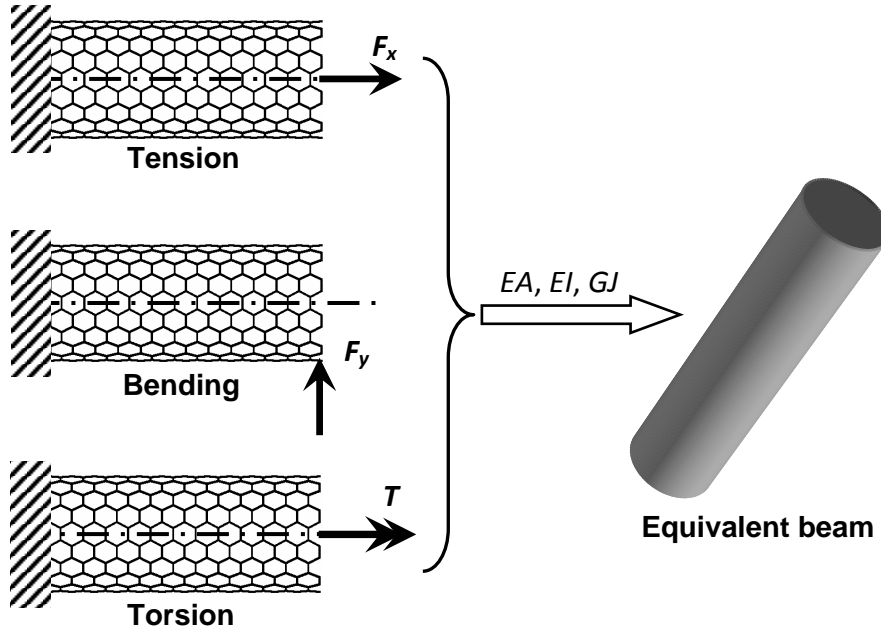


**Fig.2:** The concept of the equivalent beam.

To simulate tension, an axial displacement  $u_x$  is applied at one nanotube's end having the other end fixed. According to mechanics of materials, the axial reaction force  $F_x$  at the support is related to  $u_x$  by

$$u_x = \frac{F_x}{E_{eq} A_{eq}} L_n \quad (3)$$

where  $L_n$  is the nanotube length. The tensile rigidity is simply obtained from Eq.(3) as

$$(EA)_{eq} = \frac{F_x L_n}{u_x} \quad (4)$$

Similarly, to simulate bending, a transverse displacement  $u_y$  is applied at one nanotube's end having the other end fixed. The transverse force  $F_y$  at the support is given by

$$u_y = \frac{F_y}{3E_{eq} I_{eq}} L_n^3 \quad (5)$$

The bending rigidity is simply obtained from Eq.(5) as

$$(EI)_{eq} = \frac{F_y L_n^3}{3u_y} \quad (6)$$

To simulate torsion, a tangential force  $F_\phi$  is applied at one nanotube's end having the other end fixed. The twist angle  $\phi$  of the loaded end is related to the resulted torque  $T = F_\phi R_n$  by

$$\phi = \frac{TL_n}{G_{eq} J_{eq}} \quad (7)$$

where  $R_n$  is the nanotube radius. The torsional rigidity is simply obtained from Eq.(7) as

$$(GJ)_{eq} = \frac{TL_n}{\phi} = \frac{F_\phi R_n L_n}{\phi} \quad (8)$$

The resulted reaction forces  $F_x$  and  $F_y$  as well as the angle  $\phi$  are taken from the FE analysis.

Evaluation of the elastic moduli  $E_{eq}$  and  $G_{eq}$  and geometrical characteristics  $A_{eq}$ ,  $I_{eq}$ ,  $J_{eq}$  of the equivalent beam requires the values of the rigidities evaluated using the FE method. However, in order to provide simple relations for the equivalent beam characteristics, it was decided to fit the FE results to simple expressions using the following relations (subscript *eq* refers to the equivalent beam).

$$(EA)_{eq} = \alpha(n - n_0) \quad (9)$$

$$(EI)_{eq} = \beta(n - n_0)^3 \quad (10)$$

$$(GJ)_{eq} = \gamma(n - n_0)^3 \quad (11)$$

The parameters  $\alpha$ ,  $\beta$ ,  $\gamma$  and  $n_0$  are given in Table 1.

Parameter	Armchair	Zigzag
$\alpha$ (nN)	151.8	89.04
$\beta$ (nN nm <sup>2</sup> )	0.3469	0.0701
$\gamma$ (nN nm <sup>2</sup> )	0.3284	0.0668
$n_0$ (-)	0	0.381

**Table 1:** Values of parameters  $\alpha$ ,  $\beta$ ,  $\gamma$ ,  $n_0$

After establishing the relations between the rigidities and  $n$ , the next step is to select the profile of the equivalent beam. Obviously, due to the circular shape of the nanotube's cross-sectional area, circular profiles are more suitable. Thus, we select the solid cylindrical profile.

Consider an equivalent solid cylinder with diameter  $D_{eq}$ . Its diameter, secondary and polar moments of inertia are given by the following relations:

$$A_{eq} = \frac{\pi}{4} D_{eq}^2 \quad (12)$$

$$I_{eq} = \frac{\pi}{64} D_{eq}^4 \quad (13)$$

$$J_{eq} = \frac{\pi}{32} D_{eq}^4 \quad (14)$$

Combining Eqs.(9) and (10) with Eqs.(12) and (13)  $D_{eq}$  is derived as follows

$$\frac{(EI)_{eq}}{(EA)_{eq}} = \frac{1}{16} D_{eq}^2 = \frac{\beta}{\alpha} (n - n_0)^2 \Rightarrow D_{eq} = 4\sqrt{\frac{\beta}{\alpha}} (n - n_0) \quad (15)$$

Substituting Eq.(15) in Eqs.(12)-(14) the geometrical constants of the equivalent beam are derived as functions of the parameters  $\alpha$ ,  $\beta$  and  $\gamma$ .

$$A_{eq} = \frac{\pi}{4} D_{eq}^2 = 4\pi \frac{\beta}{\alpha} (n - n_0)^2 \quad (16)$$

$$I_{eq} = \frac{\pi}{64} D_{eq}^4 = 4\pi \left(\frac{\beta}{\alpha}\right)^2 (n - n_0)^4 \quad (17)$$

$$J_{eq} = 2I_{eq} = 8\pi \left(\frac{\beta}{\alpha}\right)^2 (n - n_0)^4 \quad (18)$$

Now, using Eqs.(9) and (11) we evaluate the elastic moduli of the equivalent beam as

$$E_{eq} = \frac{(EA)_{eq}}{A_{eq}} = \frac{\alpha^2}{4\pi\beta} (n - n_0)^{-1} \quad (19)$$

$$G_{eq} = \frac{(GJ)_{eq}}{J_{eq}} = \frac{\alpha^2\gamma}{8\pi\beta^2} (n - n_0)^{-1} \quad (20)$$

In the case of 3D modeling of the beam, the Poisson ratio is also needed

$$G_{eq} = \frac{E_{eq}}{2(1+\nu_{eq})} \Rightarrow \nu_{eq} = \frac{E_{eq}}{2G_{eq}} - 1 = \frac{\beta}{\gamma} - 1 \quad (21)$$

Eqs.(16)-(20) fully define the equivalent solid cylinder.

### 3 FE ANALYSIS OF THE RVE

The RVE is modeled as a beam with a square cross section of side  $w$ . The length of the RVE is chosen arbitrarily but long enough not to have any constraint effects. For the current work the length was chosen as  $L = 100 \text{ nm}$ . The CNT is modeled as a solid cylinder along the axis of the RVE and having the same length. The interface is modeled as a hollow cylinder with the inner diameter equal to the diameter of the CNT. In order to be consistent with the definition of the percent volume fraction used in the literature, the dimension of the RVE is chosen as follows. The volume of the CNT is considered equal to

$$V_{RVE} = w^2 L \quad (22)$$

the percent volume fraction is defined as

$$a = 100V_{CNT} / V_{RVE} = 100\pi D_n t_n L / w^2 L \Rightarrow w = \sqrt{100\pi D_n t_n / a} \quad (23)$$

which provides the dimension of the RVE. Examples of the modeled cross section of the RVE are shown in Figure 3 for  $a = 1\%$ ,  $5\%$ , and  $10\%$ .

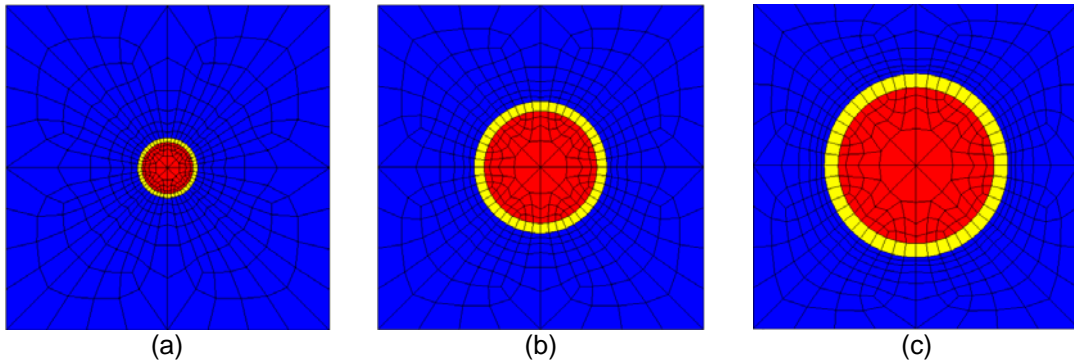


**Fig.3:** FE mesh of the cross-sectional area of the RVE indicating the matrix (blue elements), the equivalent beam representing the nanotube (red elements) and the interface (yellow).

### 4 NUMERICAL RESULTS

The properties of the matrix are assumed to be  $E = 2 \text{ GPa}$  and  $\nu = 0.35$ . The properties of the CNT are found using Eqs.(19) and (21). At the interface, variable stiffness and thickness are assigned in order to examine the effect on the tensile and bending behavior of the RVE. The RVE is subjected to tension and bending by fixing one end and apply a pre-described axial or transverse displacement at the other end. The axial or transverse reaction force is evaluated from the FE analysis. Since the size of the RVE varies with varying the volume fraction, the results are presented in the form of the corresponding rigidities.

#### 4.1 Tension

For the tension of the RVE, the important factor is volume fraction. Figure 4 plots the normalized axial rigidity  $(EA)_{RVE} / (EA)_{matrix}$  as a function of the percent volume fraction for an armchair and a zigzag nanotube. The results are for an interface stiffness of  $E_{int} = 2 \text{ GPa}$  and an interface thickness

of  $t_{int} = 0.34$  nm. A similar almost linear relation is predicted for both nanotube types. This is also verified by the rule-of-mixtures. Based on the above, it is concluded that the interface stiffness and thickness do not affect the tensile behavior of the RVE. A slight dependence is predicted in cases of very high values of the ratio between the interface and matrix stiffness.

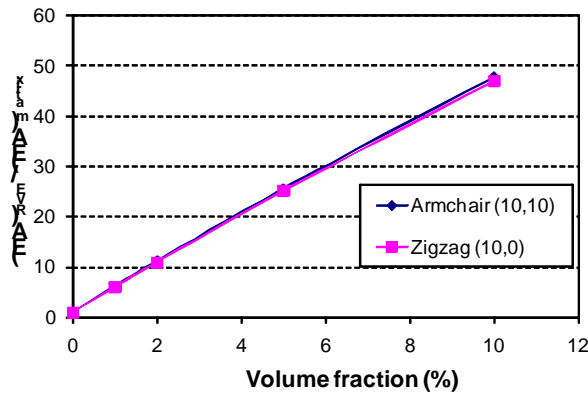


Fig.4: Axial rigidity as a function of volume fraction.

#### 4.2 Bending

For the bending loading, a non-linear effect of the percent volume fraction on the normalized bending stiffness  $(EA)_{RVE} / (EI)_{matrix}$  is predicted, as shown in Figure 5 for an armchair (10,10) nanotube with  $E_{int} = 2$  GPa and  $t_{int} = 0.34$  nm. The normalized bending stiffness is only 1.12 for 1% volume fraction reaching the value of 10 for 10%. However, this is much smaller than the normalized axial stiffness which is equal to 48 for a 10% volume fraction. This is due to the very low bending rigidity of the nanotubes as compared to their axial rigidity. A similar behavior was observed for other interface stiffness and thickness.

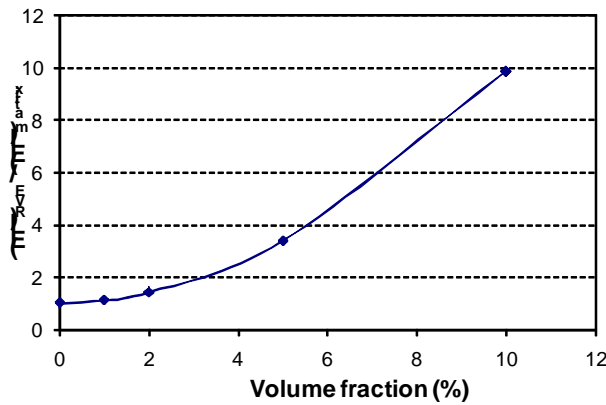
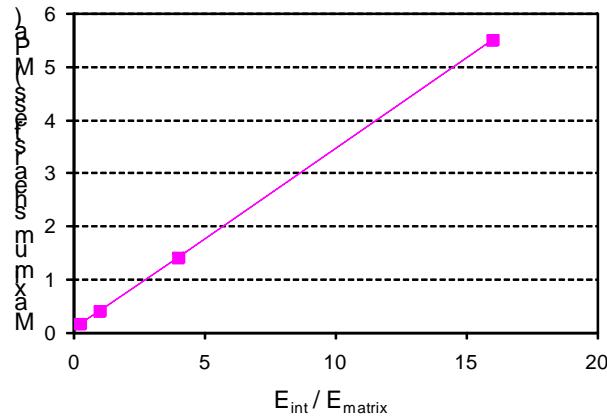


Fig.5: Bending rigidity as a function of volume fraction.

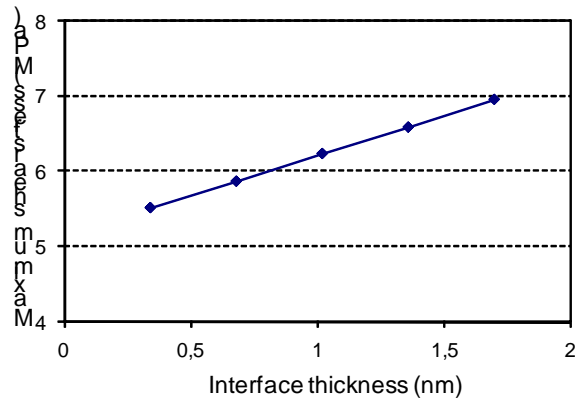
Due to bending, a high shear stress is developed at the interface, which could lead to the loss of load transfer from the nanotube to the surrounding matrix. It is therefore, important to examine how the maximum shear stress at the interface is affected by the interface thickness and stiffness.

Figure 6 shows the maximum shear stress at the interface as a function of the normalized interface stiffness  $E_{int} / E_{matrix}$  for an (10,10) armchair nanotube with 2% volume fraction and  $t_{int} = 0.34$  nm. A linear relationship is observed with the maximum shear stress reaching 5.5 MPa for  $E_{int} / E_{matrix} = 16$  ( $E_{int} = 32$  GPa). This relationship can be used to predict debonding between the nanotube and the matrix if the interfacial shear strength is known. Note that the values of interfacial shear strength reported in the literature show a very large scatter. Recently, pullout experiments performed by Cooper et al. [3] showed a scatter for the interfacial shear strength between multi-walled CNTs and epoxy matrix between 35 and 375 MPa.



**Fig.6:** Maximum shear stress at the interface as a function of interface stiffness.

The maximum interfacial shear strength as a function of interface thickness is shown in Figure 7 for an (10,10) nanotube with 2% volume fraction and  $E_{int} = 32$  GPa . Again, a linear relationship is observed.



**Fig.7:** Maximum shear stress at the interface as a function of interface thickness.

## 5 CONCLUSIONS

A parametric study on the effect of interface stiffness and thickness on tensile and bending response of CNT/polymer composites has been accomplished. For the study, a FE-based RVE has been used. For the tensile response, it was found that those two parameters do not play any role as long as both materials are loaded together. They are expected to play a minor role when pull-out loading is applied. The results also show that the bending rigidity increases with increasing the nanotube percent volume fraction. However, it still remains very small compared to tensile rigidity due to the small nanotube rigidity. Finally, a strong dependence between the maximum interfacial shear stress and the interface stiffness and thickness is ascertained in the case of bending loading. Since this stress is an indication of both load transfer between the nanotube and the matrix and initiation of interface failure, it is very important for these two interfacial parameters to be fully determined.

## REFERENCES

- [1].Desai, A.V., "Mechanics of the interface for carbon nanotube-polymer composites", *Thin-Walled Structures*, 43, 2005, 1787-1803.
- [2]. Tserpes, K.I., Papanikos, P., Labeas, G., Pantelakis, Sp., "Multi-scale modelling of the tensile behavior of carbon nanotube-reinforced composites", *Theoretical and Applied Fracture Mechanics*, In press, 2007.
- [3]. Cooper, C.A., Cohen, S.R., Barber, A.H., Wagner, H.D., "Detachment of nanotubes from a polymer matrix", *Applied Physics Letters*, 81, 2002, 3873-3875.